https://doi.org/10.26552/com.C.2012.4.26-30

Filip Pastorek – Branislav Hadzima – Pavel Dolezal *

ELECTROCHEMICAL CHARACTERISTICS OF Mg-3Al-1Zn MAGNESIUM ALLOY SURFACE WITH HYDROXYAPATITE COATING

Electrochemical characteristics of Mg-3Al-1Zn alloy surfaces after grinding and/or coating by hydroxyapatite were investigated by voltamperometric tests in 0.9 % NaCl solution. The hydroxyapatite treatments were realised by electrochemical method in water solution of $Ca(NO_3)_2 . 4H_2O$, $(NH_4)_2HPO_4$ and H_2O_2. The influences of various types of hydroxyapatite treatment processes on corrosion potentials, corrosion current densities and characteristics of passive state were evaluated. Basic potentiodynamic curves obtained from the electrochemical tests were analysed by Tafel analyses. The improvement of short-time electrochemical behaviour after hydroxyapatite treatment of tested alloy surface was reported.

1. Introduction

Traditional biomedical implant materials such as stainless steels and Ti alloys play an important role in repairing the damaged bone tissue. If these implants exist in the human body for a long time, they will always release toxic elements to impair human body's health. The application of biodegradable implants can solve this problem. The biodegradable implants can gradually be dissolved, absorbed, consumed or excreted after the bone tissue healing. Current biodegradable implants made from polymers have an unsatisfactory mechanical property [1–2]. In comparison, magnesium and its alloys are potential biodegradable materials due to their attractive biological performances [3–5]:

(1) metal magnesium is biodegradable in body fluids by corrosion;
(2) Mg^{2+} is harmless to human body;
(3) magnesium can accelerate the growth of new bone tissue;
(4) the density, elastic modulus and yield strength of magnesium are closer to the bone tissue than that of the conventional implants [2].

However, poor corrosion and fatigue resistance of magnesium and its alloys limit their applications [6–9]. Hydrogen gas evolution in the corrosion reaction causes sometimes the formation of cavities (bubbles) around the implanted alloy [4, 7]. In the case of subcutaneous gas pockets of rats, the adsorption rate of hydrogen in the tissue was determined as 0.954 $ml.h^{-1}$ based on the diffusion coefficient of hydrogen in the tissue [7]. Song et al estimated that the tolerated level of hydrogen evolution rate was 0.01 $ml.cm^{-2}.day^{-1}$ based on the size of subcutaneous bubbles in guinea pigs [3–4]. Thus, the improvement of corrosion resistance of magnesium alloys by protective coatings has been a crucial issue to promote the practical use of the alloys [10].

To reduce the biodegradation (corrosion) rate of Mg alloys, further bulk alloying is one option [5, 11–13], however this can potentially lead to the introduction of toxic elements. Biocompatible protective coatings are a practical option to moderate biodegradation allowing functional implant deployment [14]. Hydroxyapatite (HA, $Ca_{10}(PO_4)_6(OH)_2$), is a well-known biocompatible and bioactive material with close chemical and structural resemblance to human bones and teeth [15].

HA coating can be deposited on different substrates by various methods such as plasma spraying [16, 17], sputtering [18], sol–gel [19], pulse laser deposition [20], electrophoretic [21] and electrodeposition [22]. Among them, electrodeposition has received much attention due to its versatility, cost effectiveness, and ability to control the thickness and chemical composition of HA by varying the conditions employed for deposition [23–25]. Deposition of HA coating on titanium and its alloys has been studied by many researchers [23, 26, and 27]. However, the degradation behaviour of HA-coated Mg and its alloys has not been studied much [28]. Actually, some magnesium alloys containing Zr, Cd, rare earth elements and heavy metals are not suitable for biomaterials application from the medical aspect [29–30]. But the mechanical and corrosion properties of pure magnesium are unsatisfactory. In comparison with other magnesium alloys, AZ31 magnesium alloy, with low Al content, good mechanical properties and corrosion resistance, is suitable to act as biodegradable material [30]. Even though the biocompatibility of aluminium is limited [31], it

* **Filip Pastorek[1], Branislav Hadzima[1], Pavel Dolezal[2]**
[1] Department of Materials Engineering, FME, University of Zilina, Slovakia, E-mail: filip.pastorek@fstroj.uniza.sk
[2] Institute of Material Science and Engineering, FME, Brno University of Technology, Brno, Czech Republic

seems to be a valid alloying element for magnesium alloys in body contact, as it is known to diminish the magnesium corrosion rate by stabilizing hydroxides in chloride environments [32–33]. The addition of Zn to Mg alloy results in improved mechanical properties thanks to grain refinement, and shows a reduced corrosion rate compared with pure Mg [34–35].

For these reasons, the aim of this study is to electrodeposit HA coating on magnesium alloy AZ31 surface and to improve its corrosion properties this way.

2. Experimental material and methods

The tested AZ31 magnesium alloy was continually casted at Brandenburgische Universität in Cottbus, Germany and chemical composition was analysed at the Magnesium innovation centre MagIC GKSS Geesthacht, Germany. The chemical composition of AZ31 alloy is in Table 1.

Chemical composition of AZ31 alloy Table 1

Component	Al	Zn	Mn	Si	Cu	Ni	Fe	Mg
wt. %	2.96	0.828	0.433	0.004	0.004	<0.001	0.002	bal.

The samples for metallographic observation were prepared by conventional metallographic procedures. For visualization of the magnesium alloy microstructure, etchant consisting of 2.5 ml acetic acid + 2.1 g picric acid + 5 ml H_2O + 35 ml of ethanol was used [36]. The microstructure of AZ31 alloy (Fig. 1) was observed by the CARL ZEISS AXIO Imager.A1m light metallographic microscope in the laboratories of Department of Materials Engineering, University of Zilina. The microstructure is created by polyedric grains of solid solution of aluminium, zinc and other alloying elements in magnesium. The average grain size is 220 μm.

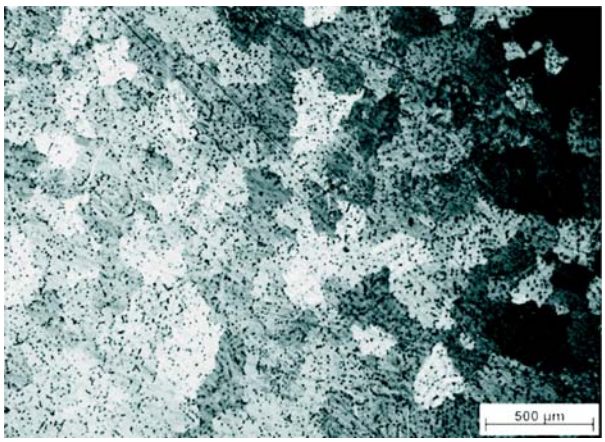

Fig. 1 Microstructure of AZ31 Magnesium alloy, light microscopy, etch. picric acid + ac. acid + ethanol + water

2.1 Experimental material surface preparation

For the evaluation of hydroxyapatite surface treatment influence on electrochemical characteristics the specimen surfaces were grinded with 1000 grit SiC paper to ensure the same surface roughness, then rinsed with demineralised water and ethanol, and dried using a stream of air. After described pre-treating the hydroxyapatite was deposed on the specimens' surfaces. Treatment electrolyte solution was prepared with 0.1 M $Ca(NO_3)_2 . 4H_2O$, 0.06 M $(NH_4)_2HPO_4$, 10 ml.l^{-1} of 30 vol.% H_2O_2. Solution pH was 4.7 and the electrodeposition was carried out at room temperature 22 ± 2 °C. Grinded AZ31 sample was used as the cathode, while a platinum electrode served as the anode. Electrodeposition was performed with constant potential 100 mV vs saturated calomel electrode (SCE) for 1 h on a laboratory apparatus VSP (producer BioLogic SAS France).

After HA deposition the surface of samples was immediately rinsed with demineralized water and dried using a stream of air and then immersed in various environments: 1 M NaOH (22±1 °C) solution for 2 h, demineralized water (22±1 °C) for 2 h and dry air (22±2 °C) for 2 h.

2.2 Experimental methods

The surface morphology of the treated samples was assessed by a stereomicroscope Nikon AZ100 with a digital camera using NIS Elements software. The corrosion characteristics of the untreated and HA-coated AZ31 in 0.9% NaCl were evaluated by potentiodynamic polarization using a potentiostat/galvanostat/frequency response analyser VSP from BioLogic SAS France. All the corrosion experiments were performed at 22±1 °C. A saturated calomel electrode and a platinum electrode served as the reference and auxiliary electrodes, respectively. Treated and untreated AZ31 samples formed the working electrode in such a way that only 1 cm² area of the working electrode surface was exposed to the electrolyte solution in corrosion cell.

Potentiodynamic polarization tests were carried out from −200 to +500 mV vs SCE with respect to the OCP (open circuit potential) at a scan rate of 1 mV.s^{-1}. Measured potentiodynamic curves were analysed using Tafel fit by EC-Lab software. The Stern and Geary equation predicts that for $E > E_{corr}$ (where E is the open circuit potential and E_{corr} is the corrosion potential) the anodic reaction predominates and that for $E < E_{corr}$ the cathodic reaction predominates [37]:

$$I \approx I_{corr} 10^{\frac{E-E_{corr}}{\beta_a}} \text{ for } E > E_{corr}$$

$$I \approx -I_{corr} 10^{\frac{E-E_{corr}}{\beta_c}} \text{ for } E < E_{corr},$$

where I is the current, I_{corr} is the corrosion current and β_a and β_c are the Tafel constants.

So, in a log I versus E representation, one should see two linear parts for $E > E_{corr}$ and $E < E_{corr}$:

$$\log I \approx \frac{E - E_{corr}}{\beta_a} + \log I_{corr} \text{ for } E > E_{corr}$$

$$\log I \approx \frac{E_{corr} - E}{\beta_c} + \log I_{corr} \text{ for } E > E_{corr}$$

The Tafel graph is displayed in log i(i is the corrosion current density) vs E where two linear regressions are automatically made using the least square method and the software deduces the corrosion potential (E_{corr}) to linear regressions intersection, the corrosion current density value (i_{corr}) and the Tafel constants (β_a and β_c) [37 and 38]. These β_a and β_c coefficients express the slope of the anodic and cathodic region of potentiodynamic polarization curve in log i vs E representation. The potentiodynamic polarization measurements were repeated at least three times so that reproducibility of the test results was ensured.

3. Results and discussion

Surface morphology after hydroxyapatite deposition is shown in Fig. 2. As can be seen, transparent irregular units with a width of 10 to 300 μm, which were homogeneously distributed throughout the sample surface, were reached by HA electrodeposition.

Fig. 3 shows the measured potentiodynamic curves of untreated and treated AZ31 Mg alloy samples using hydroxyapatite electrodeposition combined with sealing in various environments. All measured curves except the curve of non-treated surface consist of two parts. First one is a transition between an immune state and active state (characterized by corrosion potentials and corrosion current densities) and second one is a passive state of the surface finished by transpassivation potential. The curve of untreated surface has only transition between immune and active states. The thermodynamic (corrosion potentials E_{corr}, transpassive potential E_t) and kinetic (corrosion current density icorr, corrosion rate r_{corr}, anodic steady state current density in passive state i_a) characteristics obtained from the measured curves are in Table 2.

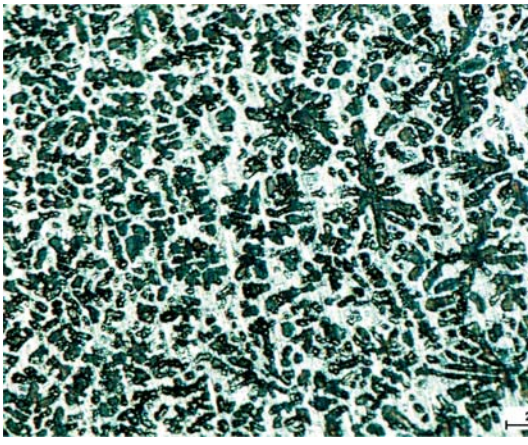

Fig. 2 Surface morphology of AZ31 after HA electrodeposition

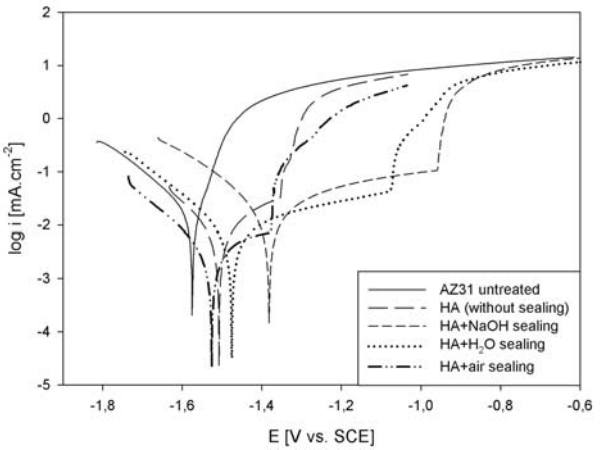

Fig. 3 Potentiodynamic curves of untreated and treated surfaces of AZ31 Mg alloy in 0.9% NaCl

Creation of the hydroxyapatite layer on the specimen's surface causes changes in both thermodynamic and kinetic characteristics. The hydroxyapatite layer is nobler and, therefore, the corrosion potential moves to more positive values. Air sealing does not change the corrosion potential; the layer is from the thermodynamic point of view similar to the layer after a hydroxyapatite process. However, the sealing in water or in 1M NaOH solution causes increase of corrosion potential values. The state is the result of magnesium hydroxide creation in pores of the hydroxyapatite layer. The thermodynamic stability of this layer is better on the surface after NaOH sealing and, therefore, the corrosion potential of this specimen reached the most positive value.

Corrosion rate in the passive state is proportional to the value of anodic steady state current density (i_a). This kinetic characteristic depends on the ability of the passive layer to slow the corrosion process. Significantly the lowest value of ia was observed on the surface of HA + air sealing samples. However, this value is reached only in a relatively narrow range of passivity ($E_t - E_{corr}$). The surface modified by HA without sealing has approximately the same value of ia as HA + H_2O sealing surface, but H_2O sealing extended interval of the layers passive behaviour nearly threefold. Sealing in 1M NaOH resulted in such changes on the HA surface that there was a substantial increase of i_a compared to the state

Electrochemical characteristics of AZ31 Mg alloy surface after various treatments Table 2

Surface treatment	E_{corr} [mV_{SCE}]	i_{corr} [$\mu A.cm^{-2}$]	r_{corr} [$mm.y^{-1}$]	i_a [$\mu A.cm^{-2}$]	E_t [mV_{SCE}]	$E_t - E_{corr}$
grinded	−1575	19.0	0.87	–	–	–
HA without sealing	−1506	5.8	0.27	~ 21	−1353	153
HA + NaOH sealing	−1381	16.8	0.77	~ 56	−957	424
HA + H_2O sealing	−1475	7.3	0.33	~ 20	−1077	398
HA + air sealing	−1526	3.0	0.14	~ 5.6	−1370	156

without sealing. A possible reason of this fact is the reduction in thickness of the HA layer by reactions running in alkaline medium. The surface is thus more protected by created $Mg(OH)_2$ areas than by an initially intended HA layer.

Another important thermodynamic indicator of corrosion resistance of material surface layers is the width of the passive state area represented by the interval between E_{corr} and E_t, where the corrosion products with a relatively good protective effect against corrosion are formed on the sample. This means that the wider this interval is, the more convenient it is. As it is shown in Fig. 3, just grinded sample does not have passive state at all. Width of the passive state of the samples HA without sealing and HA + air sealing is 153 mV and 156 mV, respectively. These nearly identical values confirm the argument that the air sealing does not change the nature of the sample's surface layer from the thermodynamic point of view. Probably a film of magnesium oxide grows on the surface that is not covered by hydroxyapatite. The largest passive state interval was measured on samples which were after HA process sealed in H2O (398 mV) and NaOH (424 mV). These environments were able to create Mg hydroxides on the sample`s surface which are stable even at higher potential.

The third important electrochemical characteristic is the corrosion current density i_{corr} that assesses the corrosion process in terms of kinetics. It is proportionally related to the corrosion rate rcorr that expresses weight losses of material in certain environment over time. The highest and, therefore, in terms of corrosion the least desirable current density value (i_{corr} = 19 $\mu A.cm^{-2}$) was obtained on just grinded surface. The process of HA caused decrease by two thirds compared with just grinded samples that is reflected in two thirds reduction of corrosion rate. Formed HA layer thus largely contributes to slowing the corrosion process. The use of an additional sealing in H_2O and thus creation of protective magnesium hydroxides in this way had no additive effect on further reduction of the corrosion current density (i_{corr} = 7.3 $\mu A.cm^{-2}$). On the contrary, sealing in NaOH after HA process caused dissolution of created HA layer and formation of Mg hydroxides on the sample's surface. It resulted in an increase of the corrosion current density to values approaching those obtained for just grinded samples.

Overall, the lowest value of i_{corr} was reached at HA + air sealing samples where the air filled the gaps in HA by MgO oxides which resulted in reducing the corrosion current density by half compared with the HA samples without sealing.

5. Conclusions

On the basis of the measured data and analyses we concluded:

1. The bioactive hydroxyapatite (HA) coating was successfully obtained by electrodepostion on magnesium alloy AZ31 to improve in combination with different sealings the corrosion properties of the surface.
2. The highest Ecorr value and the widest passive state interval were reached by treatment process consisted of HA + NaOH sealing and the lowest current density was measured at HA + air sealing samples.
3. Taking into account electrochemical corrosion resistance criteria (thermodynamic and kinetic), the most appropriate process consisting of HA electrodeposition and H_2O sealing was considered.

Acknowledgements

The research is supported by the European regional development fund and Slovak state budget by the project ITMS 26220220048 (call OPVaV-2008/2.2/01-SORO). The authors are grateful for the support in experimental works to project VEGA No. 1/0100/11.

References

[1] LIU, C. L., XIN, Y. C., TANG, G. Y.: *Mater. Sci. Eng.* A 456, 2007, 350–357.
[2] SONG, Y. W., SHAN, D. Y., HAN, E. H.: *Mater. Lett.* 62, 2008, 3276–3279.
[3] SONG, G.L.: *Corr. Sci.* 49, 2007, 1696–1701.
[4] WITTE, F., KAESE, V., HAFERKAMP, H.: *Biomater.* 26, 2005, 3557–3563.

[5] WITTE, F., FISCHER, J., NELLESEN, J.: *Biomater.* 27, 2006, 1013–1018.
[6] HADZIMA, B., PALCEK, P.: *Mater. Eng - Mater. inz.* 8, 2001, 67–74.
[7] WITTE, F., HORT, N., VOGT, C., COHEN, S., KAINER, K.U., WILLUMEIT, R., FEYERABEND, F.: *Curr. Opin. Solid State Mater. Sci.* 12 (5–6), 2008, 63–72.
[8] STAIGER, M.P., PIETAK, A.M., HUADMAI, J., DIAS, G.: *Biomater.* 27, 2006, 1728–1734.
[9] NOVY, F., JANECEK, M., SKORIK, V., MULLER, J., WAGNER, L.: *Int. J. Mater. Res.* 100, 2009, 288–291.
[10] HIROMOTO, S., TOMOZAWA, M.: *Surf. Coat. Technol.* 205, 2011, 4711–4719.
[11] KIRKLAND, N.T., LESPAGNOL, J., BIRBILIS, N., STAIGER, M.P.: *Corr. Sci.* 52, 2010, 287–291.
[12] BIRBILIS, N., EASTON, M. A., SUDHOLZ, A. D., ZHU, S.M., GIBSON, M. A.: *Corr. Sci.* 51, 2009, 683–689.
[13] GU, X.-N., ZHENG, Y.-F., CHENG, Y., ZHONG, S.-P., XI, T.-F.: *Biomater.* 30, 2009, 484–498.
[14] GRAY, J. E., LUAN, B.: *J. Alloys Compd.* 336, 2002, 88–113.
[15] CHEN, X.-B., BIRBILIS, N., ABBOTT, T. B.: *Corr. Sci.* 53, 2011, 2263–2268.
[16] SOUTO, R. M., MARIA, M. L., RUI, L. R.: *Biomater.* 24 (23), 2003, 4213–4221.
[17] SOUTO, R. M., MERCEDES, M. L., REIS, R. L.: J. *Biomed. Mater. Res.* 70A (1), 2004, 59–65.
[18] YAMAGUCHI, T., TANAKA, Y., IDE-EKTESSABI, A.: *Nucl. Instrum. Methods* B 249 (1–2), 2006, 723–725.
[19] AKSAKAL, B., GAVGALI, M., DIKICI, B.: *J. Mater. Eng. Perform.* 19 (6), 2004, 894–899.
[20] MAN, H. C., CHIU, K. Y., CHENG, F. T., WONG, K. H.: *Thin Solid Films* 517 (18), 2009, 5496–5501.
[21] YOUSEFPOUR, M., AFSHAR, A., CHEN, J., ZHANG, X.: *Mater. Sci. Eng.* C, 27 (5–8), 2007, 1482–1486.
[22] KAR, A., RAJA, K. S., MISRA, M.: *Surf. Coat. Technol.* 201 (6), 2006, 3723–3731.
[23] SOBIESZCZYK, S.: *Adv. Mater. Sci.* 10 (1), 2010, 19–28.
[24] LIU, X., CHU, P. K., DING, C.: *Mater. Sci. Eng.* R47 (3–4), 2004, 49–121.
[25] SAMEER, R. P., NARENDRA, B. D.: *Mater. Sci. Eng.* R66 (1–3), 2009, 1–70.
[26] BAN, S., HASEGAWA, J.: *Biomater.* 23 (14), 2002, 2965–2975.
[27] HU, H. B., LIN, C. J., HU, R., LENG, Y.: *Mater. Sci. Eng.* C20 (1–2), 2002, 209–214.
[28] JAMESH, M., KUMAR, S., SANKARA NARAYANAN, T. S. N.: *J. Coat. Technol. Res,* 2011, DOI 10.1007/s11998-011-9382-6 (on-line).
[29] SONG, G. L.: *Corr. Sci.* 49, 2007, 1696.
[30] SONG, Y., SHAN, D., CHEN, R., ZHANG, F., HAN, E. H.: *Mater. Sci. Eng.* C29 (3), 2009, 1039–1045.
[31] LOTHAR, T.: *Labor und Diagnose,* 5th ed., TH-Books, Frankfurt 2000.
[32] HADZIMA, B., BUKOVINA, M., DOLEZAL, P.: *Mater. Eng. - Mater. inz.* 17(4), 2010, 14–19.
[33] WITTE, F., KAESE, V., HAFERKAMP, H., SWITZER, E., MEYER-LINDENBERG, A., WIRTH, C. J.: *Biomater.* 26, 2005, 3557–3563.
[34] DAS, A., LIU, G., FAN. Z.: *Mater. Sci. Eng.* A419 (1-2), 2006, 349–356.
[35] KIRKLAND, N. T., STAIGER, M. P., NISBET, D., DAVIES, C. H. J., BIRBILIS, N. B.: *JOM* 63(6), 2011, 28-34.
[36] ASM Handbook, vol 9: *Metallography and Microstructures.* Ed: VANDER VOORT, G.F., ASM International, New York, 2004.
[37] EC-Lab Software User's Manual, version 10.1x – February 2011.
[38] LIPTAKOVA, T.: *Pitting Corrosion of Stainless Steels (in Slovak),* EDIS ZU v Ziline, 2009.